

Differential pressure difference based altitude control of a stratospheric satellite^①

CHEN Li (陈 丽)^{②*}, WANG Xiaoliang^{**}

(* Flight College, Shanghai University of Engineering Science, Shanghai 201620, P. R. China)

(** School of Aeronautics and Astronautics, Shanghai Jiao Tong University, Shanghai 200240, P. R. China)

Abstract

An autonomous altitude adjustment system for a stratospheric satellite (StratoSat) platform is proposed. This platform consists of a helium balloon, a ballonet, and a two-way blower. The helium balloon generates lift to balance the platform gravity. The two-way blower inflates and deflates the ballonet to regulate the buoyancy. Altitude adjustment is achieved by tracking the differential pressure difference (DPD), and a threshold switching strategy is used to achieve blower flow control. The vertical acceleration regulation ability is decided not only by the blower flow rate, but also by the designed margin of pressure difference (MPD). Pressure difference is a slow-varying variable compared with altitude, and it is adopted as the control variable. The response speed of the actuator to disturbance can be delayed, and the overshoot caused by the large inertia of the platform is inhibited. This method can maintain a high tracking accuracy and reduce the complexity of model calculation, thus improving the robustness of controller design.

Key words: stratospheric satellite (StratoSat), differential pressure difference (DPD), altitude adjustment, threshold switching strategy, margin of pressure difference (MPD)

0 Introduction

Static lift aerial vehicles have been proposed as environment monitoring platforms due to their hovering ability^[1]. For environment monitoring, atmospheric experiments require sensor readings across a wide range of altitudes, so autonomous altitude regulation is necessary to continue flying at different altitudes^[2-3].

The general structure of the majority of existing static lift aerial vehicles is a balloon equipped with ballast, valves and a one-way blower^[4]. Altitude adjustment is achieved indirectly by adjusting the buoyancy by changing the ballast weight or inflating the ballonet by using blower^[5-7]. In these methods, accurate altitude control cannot be obtained for lacking the relationship of altitude with the buoyancy. During ascent and descent, the temperature and pressure variations are nonlinear time-varying functions of altitude. To date, no adequate knowledge or data on thermal characteristics are available to establish an elaborate thermody-

amic model of scientific balloons^[8-10], so accurate altitude control for balloons is difficult. Thus, less research has been conducted on the elaborate altitude control of balloons compared with the research on altitude control of airships^[11-13]. Airships, like balloons, have a main balloon and ballonets, but their altitude control methods involve not only buoyancy, but also elevator surfaces, moving masses, and vector thrusters^[14-16].

Most of the existing altitude control methods for static lift aerial vehicles are designed based on vertical acceleration dynamic equations directly and adopt complex algorithms to accommodate model errors^[17-19]. Some researchers have worked on artificial intelligence (AI) to realize the model-free control of complex air vehicles^[20]. However, the training data that AI relies on are from experimental data, which increases the complexity of controller design.

Stratospheric satellite (StratoSat) proposed in this paper is a long-life balloon that flies at 20 km altitude in near-space. The buoyancy changes by inflating and deflating the ballonet via a two-way blower hanging un-

① Supported by the National Natural Science Foundation of China (No. 52175103).

② To whom correspondence should be addressed. E-mail: cl200432@tom.com.

Received on June 16, 2023

der the platform. Altitude adjustment is achieved by tracking the differential pressure difference (DPD), and a threshold switching strategy is used to achieve blower flow control. For the pressure difference at given altitude can be accurately measured by sensors, so this method can maintain a relatively high tracking accuracy, and the reliability of control system is guaranteed by avoiding a complex dynamic model and control algorithm.

This paper is organized as follows. Section 1 introduces the platform net lift model. Section 2 gives parameter design of the StratoSat. Section 3 presents the general controller structure. In Section 4, a simulation is implemented, and the results are discussed. In Section 5, a brief summary is provided, and future work directions are put forward.

1 Net lift model of StratoSat

This platform consists of a helium balloon, a ballonnet, and a two-way blower, as shown in Fig. 1. The main balloon is filled with helium. A two-way blower is installed at the bottom of the ballonnet, and it can realize the inflation and deflation of the ballonnet and achieve air mass changes by controlling the flow rate of the blower (air mass change per second in ballonnet). The static model of this platform is given as follows.

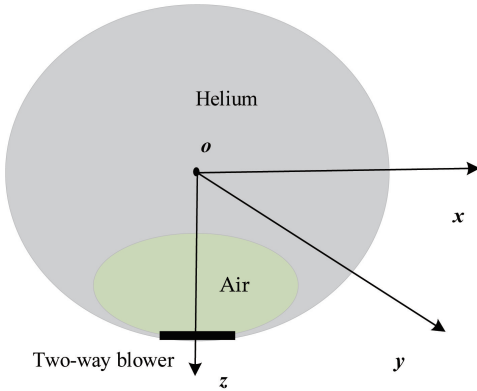


Fig. 1 General structure of the StratoSat

The total mass composition of the platform is

$$m = m_{\text{struc}} + m_h + m_a \quad (1)$$

where m_{struc} is the structure mass, m_a is the ballonnet mass, and m_h is the helium mass.

The platform satisfies the maximum volume constraint, maximum pressure difference constraint, and constant helium mass condition. For a given altitude, it has:

$$\begin{aligned} m_a &= \rho_a V_a \left(1 + \frac{\delta P_a}{P}\right) \\ m_h &= \rho_h V_h \left(1 + \frac{\delta P_h}{P}\right) \\ V &= V_a + V_h \\ \delta P_a &= P \left(\frac{m_a}{2 \rho_a V_a} - 1\right) \\ \delta P_h &= P \left(\frac{m_h}{\rho_h V_h} - 1\right) \end{aligned} \quad (2)$$

where δP_h and δP_a are the pressure difference between the internal and external pressures of the helium balloon and the ballonnet, respectively; ρ_a and V_a are the air density and volume of the ballonnet, respectively; ρ_h and V_h are helium density and helium balloon volume, respectively; P is the pressure of the external reference atmosphere; and V is the total volume of the platform.

The net lift (NL) F_{nl} of the platform is

$$F_{\text{nl}} = B - G = \rho g V - mg \quad (3)$$

where B and G represent the buoyancy and gravity of the platform, respectively; ρ is the density of the external reference atmosphere. The detailed NL model generated by the whole platform is

$$\begin{aligned} F_{\text{nl}} &= g \left[(\rho_a - \rho_h (1 + \delta P_h / P)) V_h \right. \\ &\quad \left. + (\rho_a - \rho_a (1 + \delta P_a / P)) V_a \right] \\ &= g \left[(\rho_a - \rho_h) V_h - \rho_h \frac{\delta P_h}{P} V_h - \rho_a \frac{\delta P_a}{P} V_a \right] \\ &\quad - m_{\text{struc}} g \end{aligned} \quad (4)$$

where g is the gravitational acceleration.

The traditional pressure difference altitude control of aerostat is a kind of passive control^[21-22]. Within a reasonable range of pressure difference, deflating or inflating the ballonnet by using valve or blower to change the net lift of the aerostat can change altitude, as shown in Eq. (4). However, this method can not control the balloon to reach the specified altitude, as the relationship between the differential pressure and altitude is unknown, and there is no continuous pressure difference measurement, only the maximum and minimum differential pressure is designed without its limits.

2 Parameter design of the StratoSat

The platform parameters are designed for the task of environment monitoring. Suppose the platform's maximum hovering altitude is 20 km, and the structure mass is $m_{\text{struc}} = 236.5$ kg. The pressure difference at 20 km is designed to be $\delta P_a = \delta P_h = 200$ Pa. The maximum pressure difference for the balloon is $\Delta P_{\text{max}} = 500$ Pa. If the diameter of this platform is 20 m, then the overall volume would be $V = 4188 \text{ m}^3$. Under the

lift and gravity balance condition at 20 km, the total volume remains the same:

$$\begin{cases} g[(\rho_a - \rho_h)V_h - \rho_h \frac{\delta P_h}{P} V_h - \rho_a \frac{\delta P_a}{P} V_a] \Big|_{h=20 \text{ km}} \\ - m_{\text{struc}}g = 0 \\ V_h + V_a \Big|_{h=20 \text{ km}} = V \end{cases} \quad (5)$$

The calculation results are $V_a = 1\,041$, $V_h = 3\,147$, then $m_h = 40$ kg and $m_a = 96$ kg are obtained at 20 km for balance. It is assumed that there is no gas exchange during the ascent process, so at the initial altitude of 10 m, the helium mass and air mass are the same as at 20 km altitude. Then the obtained buoyancy at 10 m is 13 kg, which achieves the initial ascent.

The blower design provides the maximum amount of inflation and deflation that can be achieved in a control cycle, which is the design basis for pressure difference change threshold (PDT) δ . For this platform, the control period is set to 1 s, and PDT of $2 \text{ Pa} \cdot \text{s}^{-1}$ is designed, then maximum flow rate of the blower is below $0.8 \text{ kg} \cdot \text{s}^{-1}$ at arbitrary altitude; this is reflected in subsequent simulations. Overall parameters of the platform is shown in Table 1.

Table 1 Parameters of the platform

Parameters	Value
Initial altitude	10 m
Total platform volume	4 188 m ³
Initial helium mass	40 kg
Initial ballonnet mass	96 kg
Helium volume at 10 m	237 m ³
Ballonnet volume at 10 m	78 m ³
Pressure difference at 20 km	200 Pa
Maximum pressure difference	500 Pa
Structure mass	236.5 kg
Buoyancy at 10 m altitude	13 kg
Gravity center position	4 m
Flow rate of the blower	$0.8 \text{ kg} \cdot \text{s}^{-1}$
Pressure difference change threshold	$2 \text{ Pa} \cdot \text{s}^{-1}$

3 General controller structure

Complex controller algorithms are unsuitable for engineering applications because achieving an accurate

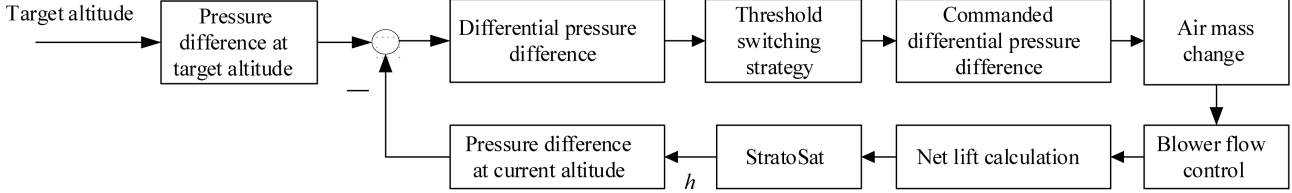


Fig. 2 General controller structure

dynamic model is difficult, so this study proposes an altitude adjustment method based on DPD. This controller design is simply implemented by avoiding the trouble of accurate modeling, and it is convenient for adoption in practical controller design. The controller structure is shown in Fig. 2.

Closed-loop altitude control begins when the platform reaches the maximum altitude of 20 km, there is a pressure difference between the inside and outside of the balloon. Thus, the platform has a fixed shape, and its volume is at the maximum value. This is defined as the steady state of the platform. Assume that the pressure difference of the helium balloon and ballonnet is equal under the steady state for a given station keeping altitude, which means the shape may be changed during the height adjustment process. For the platform in steady state, the volume ratio k of the helium balloon to the ballonnet is fixed. Volume ratio k can be deduced from Eq. (6).

$$k = \frac{m_h \rho_a}{m_a \rho_h} \quad (6)$$

$$V_a = V / (1 + k)$$

$$V_h = V - V_a$$

The pressure difference δP_{at} at the target altitude (TA) and the pressure difference δP_{ah} at the current altitude (CA) can be deduced from the lift and gravity balance condition at different altitudes, respectively, as shown in Eqs (7) and (8).

$$\delta P_{\text{at}} = \frac{P[(\rho_{\text{at}} - \rho_{\text{ht}})V_{\text{ht}} - m_{\text{struc}}]}{\rho_{\text{ht}}V_{\text{ht}} + \rho_{\text{at}}V_{\text{at}}} \quad (7)$$

$$\delta P_{\text{ah}} = \frac{P[(\rho_a - \rho_h)V_h - m_{\text{struc}}]}{\rho_h V_h + \rho_a V_a} \quad (8)$$

where ρ_{at} and V_{at} are the air density and volume of the ballonnet at TA, respectively, and ρ_{ht} and V_{ht} are helium density and volume of the helium balloon at TA, respectively.

The DPD between CA and TA is calculated as

$$\Delta = \delta P_{ah} - \delta P_{at} \quad (9)$$

The ballonnet tracking pressure difference δP_{ac} is determined by Δ by using a threshold switching strategy. Δ is compared with a threshold δ , which is defined in the system design phase. If Δ is less than δ , then the target pressure difference is assigned directly to the tracking pressure difference; if Δ exceeds δ , then the tracking pressure difference is the current pressure difference plus or minus the threshold δ depending on the sign of Δ . This tracking commanded differential pressure difference assignment logic is

$$\begin{cases} \delta P_{ac} = \delta P_{at} & |\Delta| < \delta \\ \delta P_{ac} = \delta P_{ah} - \delta & \Delta > \delta \\ \delta P_{ac} = \delta P_{ah} + \delta & \Delta < -\delta \end{cases} \quad (10)$$

On the basis of the condition that the pressure difference between the helium balloon and ballonnet is equal ($\delta P_{hc} = \delta P_{ac}$), the helium pressure difference tracking command is obtained. It is assumed that only the ballonnet has gas exchange during the altitude adjustment process, and the required helium balloon volume is calculated through the conservation of helium mass. Then, the ballonnet volume is derived from the invariant total volume. Based on the helium mass conservation, it can be derived as

$$V_{hc} = \frac{m_h}{\rho_h \left(1 + \frac{\delta P_{hc}}{P}\right)} \quad (11)$$

$$V_{ac} = V - V_{hc}$$

where V_{hc} and V_{ac} are the commanded volumes to be reached.

The required mass change of the ballonnet is calculated according to the tracking pressure difference command. Then, the remaining air mass of the ballonnet is

$$m_{ac} = \rho_a V_{ac} \left(1 + \frac{\delta P_{ac}}{P}\right) \quad (12)$$

The change in air mass is calculated as

$$\Delta m = m_a - m_{ac} \quad (13)$$

A two-way blower realizes the inflation and deflation of the ballonnet and achieves these air mass changes by controlling the size of the blower flow.

The net lift (NL) of the platform, F_{nl} , is deduced from Eq. (4), in which the direct control variables act on the aerial platform (AP) to overcome structure gravity and regulate the altitude. The DPD based threshold switching strategy of tracking control is shown in Fig. 3.

In this scheme, the control strategy can be worked out without access to an accurate dynamic model. Only the pressure difference at different altitudes needs to be determined. In Eq. (7), the volume ratio at TA is un-

known, so the volume ratio at CA in Eq. (8) is used to calculate ballonnet volume V_{at} and helium balloon volume V_{ht} at TA. This volume ratio gradually approaches the target one as the platform approaches TA.

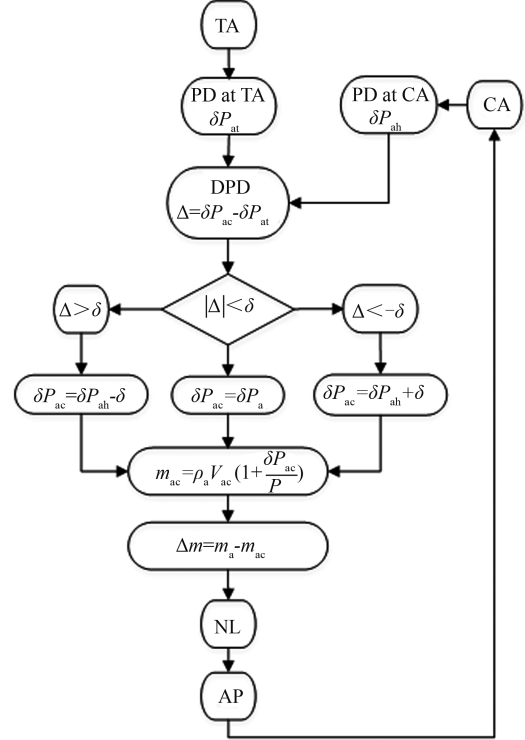


Fig. 3 DPD based threshold switching strategy

4 Altitude regulation validation

4.1 Mass dynamics

The attitude of the platform is assumed to be small and can be ignored. The mass model of the platform is established in the body frame for simulation as follows.

$$\begin{cases} a_x = \frac{D_x}{m} \\ a_y = \frac{D_y}{m} \\ a_z = -\frac{B - G - D_z}{m} \end{cases} \quad (14)$$

where a_x , a_y , a_z are the accelerations; the external force in the body frame are buoyancy B , gravity G and aerodynamic drag components D_x , D_y , and D_z , they are expressed as

$$\begin{aligned} D_x &= \frac{1}{2} \rho |w_x - v_x| (w_x - v_x) S_{ref} c_x \\ D_y &= \frac{1}{2} \rho |w_y - v_y| (w_y - v_y) S_{ref} c_y \\ D_z &= \frac{1}{2} \rho |w_z - v_z| (w_z - v_z) S_{ref} c_z \end{aligned} \quad (15)$$

where S_{ref} is the reference area, which is equal to the

cross-sectional area of the sphere; the isotropic aerodynamic drag coefficients are $c_x = c_y = c_z = 0.5$; v_x, v_y, v_z refer to the ground speed; and w_x, w_y, w_z refer to the wind speed.

4.2 Simulation results

The simulation is divided into three phases: open ascending, autonomous descending, and autonomous ascending. The target altitude is designed as

$$h_i = \begin{cases} 20 \text{ km} & 0 \leq t < 8\,000 \\ 10 \text{ km} & 8\,000 \leq t < 15\,000 \\ 15 \text{ km} & 15\,000 \leq t < 20\,000 \end{cases} \quad (16)$$

The simulation of the entire process of the platform is given in Figs 4 – 8. In Fig. 4, h is the altitude of the platform, δP_a is the pressure difference of the ballonet, dm_a is the flow rate of blower in the ballonet, dw is the vertical acceleration of the platform.

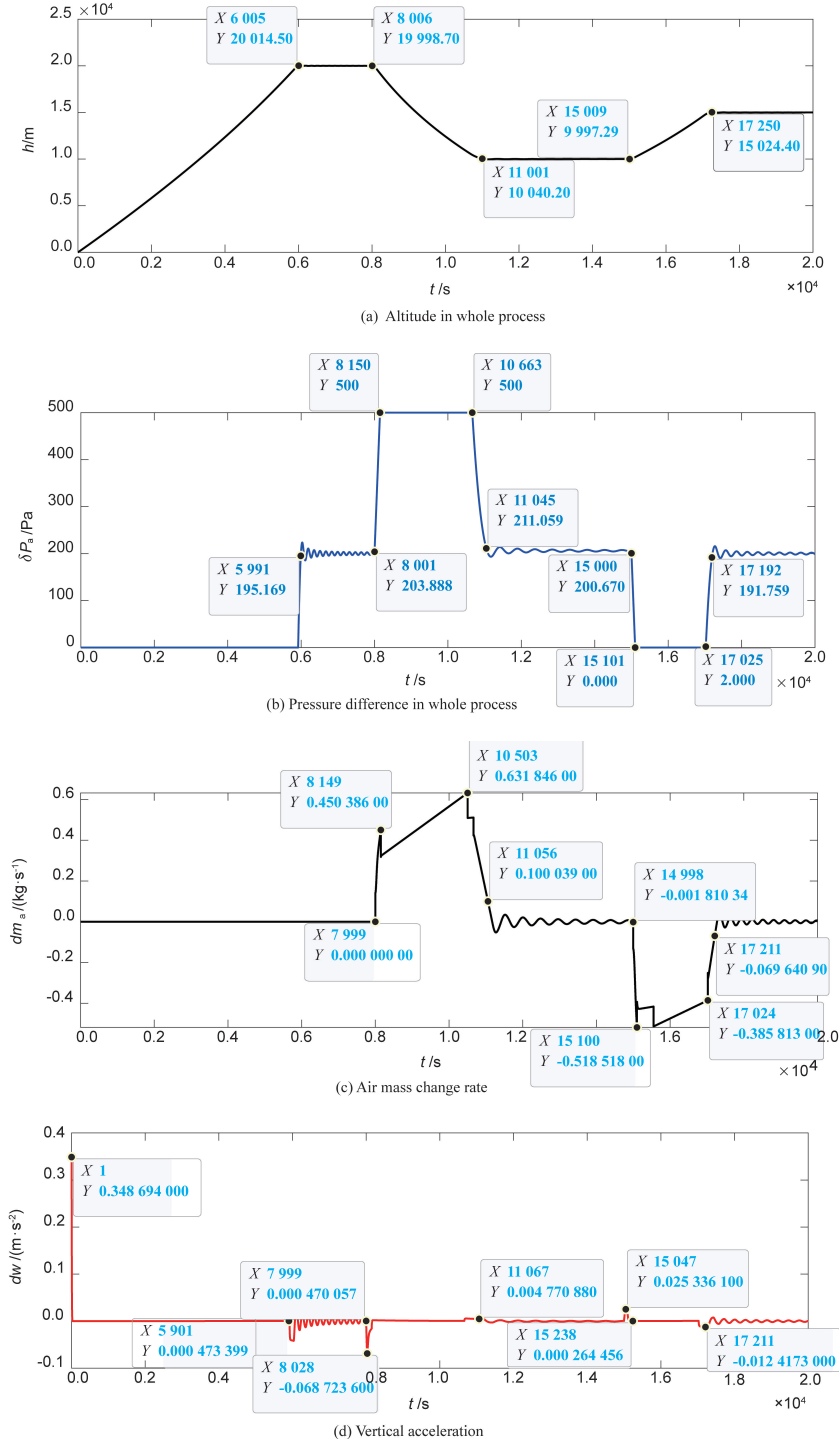


Fig. 4 Altitude and control variables in whole process

In Fig. 5, m_a is the air mass of the ballonnet, V is the total volume of the platform, V_h is the volume of the helium balloon, and V_a is the volume of ballonnet.

In Fig. 6, B is the total buoyancy of the platform, Dz is the drag in the vertical direction, δP_{he} is pressure difference of the helium balloon and w is the vertical speed of the platform.

In the first flight phase, the platform filled with a certain amount of air and helium rises from the ground and reaches an altitude of 20 km (Fig. 4(a)) at 6 000 s, which is the limit altitude designed for the platform. The pressure difference is 200 Pa (Fig. 4(b)). The helium and air fill the entire volume, and the platform is in an over-pressured steady state (Fig. 5(b)). The helium balloon volume is 3 124 m³, and the ballonnet volume is 1 040 m³ (Fig. 5(c), (d)). The initial ascend-

ing rate of the platform is 0.35 m · s⁻¹ and reaches 2.77 m · s⁻¹ at 30 s (Fig. 6(d)). At the same time, the vertical drag also increases to 131 N (Fig. 6(b)); the maximum ascending speed is 4.26 m · s⁻¹ at 5 919 s (Fig. 6(d)), at the same time the pressure difference is generated from 5 919 s. Then, the ascent speed begins to decrease (Fig. 6(c)), and the platform speed decreases to 0 from 5 919 s to 5 997 s; afterward, it stabilizes at a stationary altitude for a period of time.

The second descending phase begins at 8 000 s. The target altitude is 10 km, and it is achieved by inflating the ballonnet and increasing the weight of the platform. The platform reaches 10 km at 11 001 s (Fig. 4(a)); the helium volume is 695 m³ (Fig. 5(c)), and the ballonnet volume is 3 493 m³ (Fig. 5(d)). The

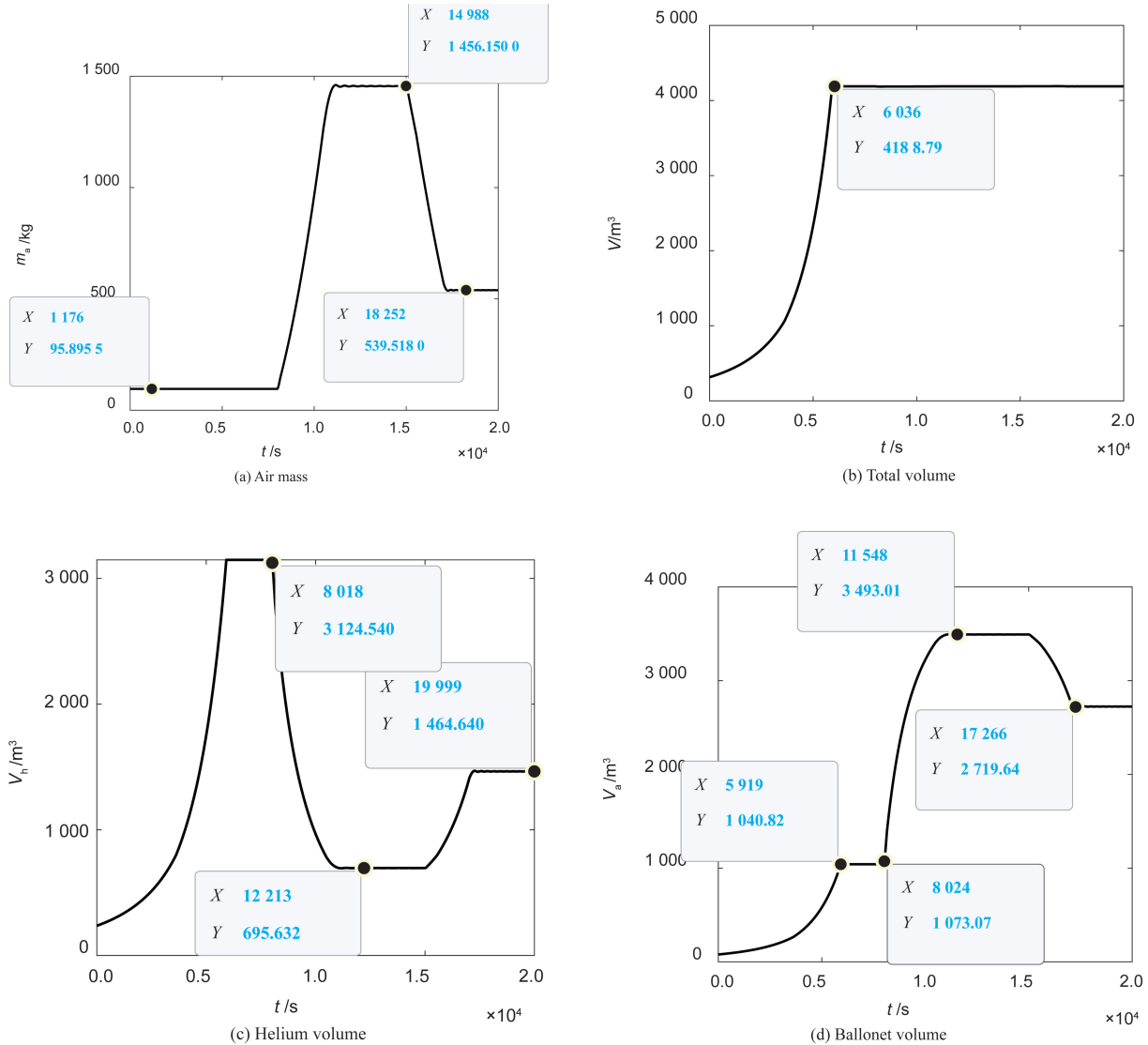


Fig. 5 Remaining air mass and volume in whole process

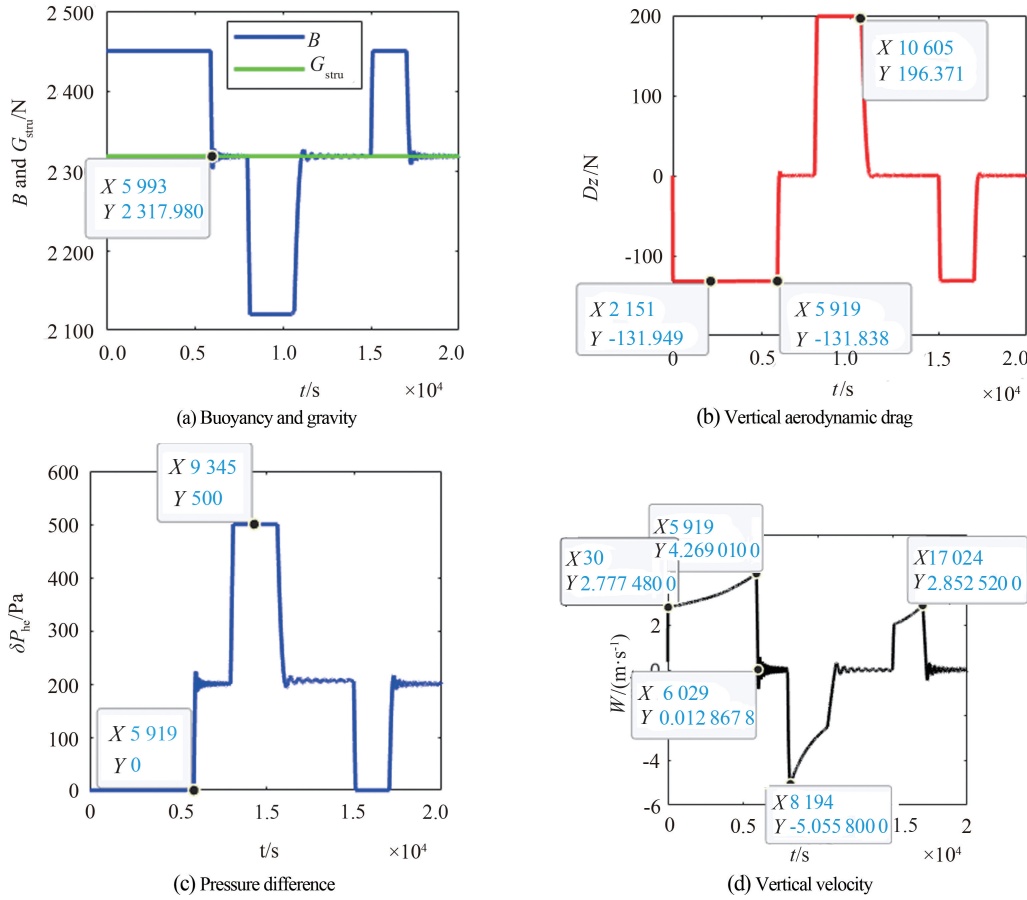


Fig. 6 Force, pressure difference and vertical velocity of the platform

maximum descent speed is $-5.05 \text{ m} \cdot \text{s}^{-1}$ (Fig. 6(d)), and the maximum descent acceleration is $-0.0687 \text{ m} \cdot \text{s}^{-2}$ (Fig. 4(d)). The steady-state pressure difference is light damping oscillated up and down at around 200 Pa (Fig. 4(b)). The air mass is 1456 kg at a stable altitude (Fig. 5(a)), and the pressure difference during the descent process reaches a limit value of 500 Pa (Fig. 4(b)) from 8001 s to 8150 s. The flow rate of the blower occurs at 8150 s with $0.450 \text{ kg} \cdot \text{s}^{-1}$ (Fig. 4(c)), which is corresponding to maximum descent acceleration $-0.0680 \text{ m} \cdot \text{s}^{-2}$ (Fig. 4(d)); the maximum flow rate is $0.631846 \text{ kg} \cdot \text{s}^{-1}$ at 10503 s, when the pressure difference of ballonnet is 500 Pa (Fig. 4(b)).

The third ascending phase begins at 15000 s. The target altitude is 15 km, and the weight of the platform is reduced by ballonnet deflation, which is constrained by the minimum pressure difference of 0 Pa. The platform reaches this altitude in 17250 s (Fig. 4(a)) with a helium volume of 1464 m^3 (Fig. 5(c)) and a ballonnet volume of 2719 m^3 (Fig. 5(d)). The maximum ascent speed is $2.85 \text{ m} \cdot \text{s}^{-1}$ (Fig. 6(d)). The steady state pressure difference is light damping oscillated up and down at around 200 Pa (Fig. 4(b)), and the air mass is 539 kg at a stable altitude (Fig. 5(a)). The

maximum flow rate of the blower during the ascent process occurs at 15100 s with $-0.518 \text{ kg} \cdot \text{s}^{-1}$ (Fig. 4(c)), which is corresponding to the maximum ascent acceleration $0.0253 \text{ m} \cdot \text{s}^{-2}$ (Fig. 4(d)).

Furthermore, different target altitudes are set to validate the altitude regulation ability as shown in Figs 7–8. In this simulation, with different descending target altitudes in the second phase, shown as $TA = 9000, TA = 10000, TA = 13000$, the remaining air masses are different with different TAs, as shown in Fig. 6. However variations of other control variables change with the same regularities; with different TAs, the control durations are different, as shown in Fig. 7.

From above simulation results, it can be seen that arbitrary altitude regulation is obtained with this simple control logic shown in Fig. 3. Given different TAs, the maximum flow rate is $0.630 \text{ kg} \cdot \text{s}^{-1}$, which satisfies the design condition of $0.800 \text{ kg} \cdot \text{s}^{-1}$ as shown in Table 1. The control variable in this scheme is DPD, which is a slow-varying variable. The control response to differential pressure difference is delayed, and the overshoot caused by the large inertia of the platform is inhibited (Fig. 7(a)).

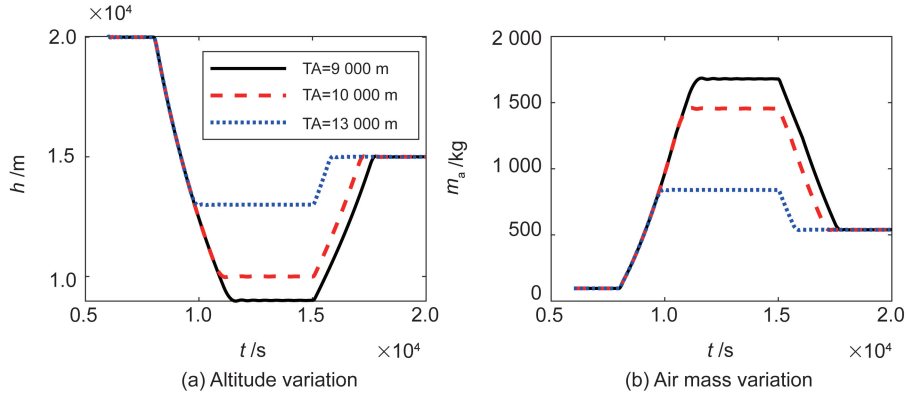


Fig. 7 Different TAs and remaining air mass

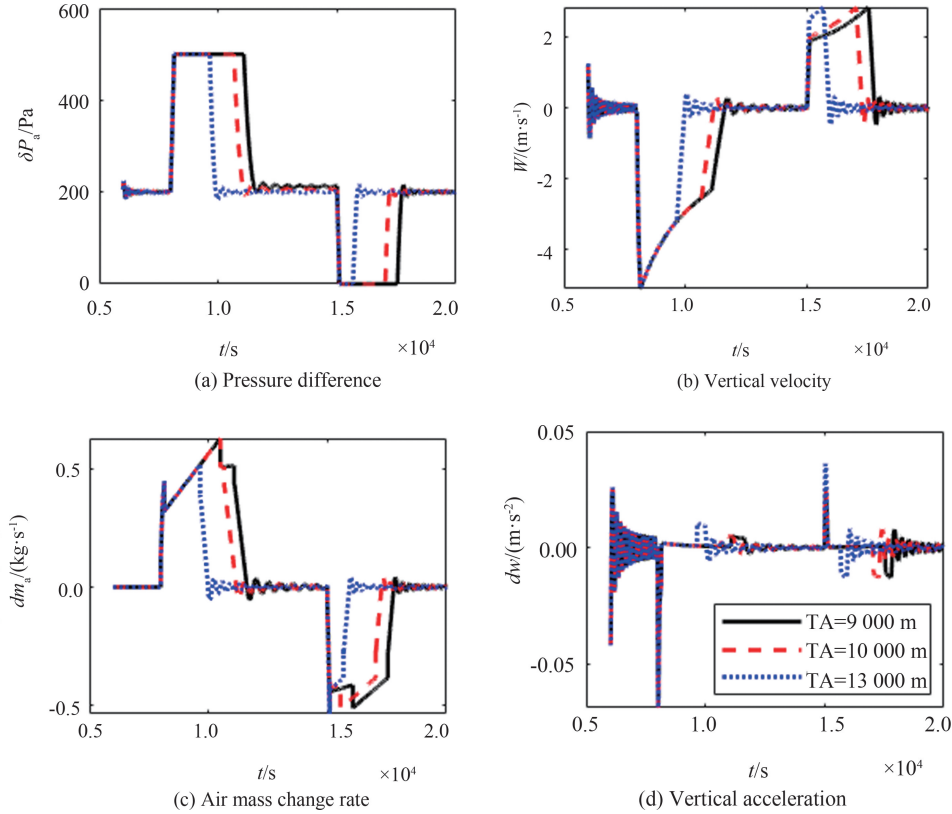


Fig. 8 State variations with different TAs

4.3 Further discussion

4.3.1 Constant pressure difference at station-keeping altitude

In descent phase from 8 000 s to 11 000 s (Fig. 4(a)), the pressure difference of ballonnet is increasing from 200 Pa to 500 Pa, then decreasing to 200 Pa (Fig. 4(b)). In ascent phase from 15 000 s to 17 000 s (Fig. 4(a)), the pressure difference of ballonnet is decreasing from 200 Pa to 0 Pa, then increasing to 200 Pa (Fig. 4(b)). The designed pressure difference at 20 km is $\delta P_a = \delta \rho_h = 200$ Pa. The pressure difference between the helium balloon and ballonnet varies during the altitude adjustment process, but

it reaches the designed value of 200 Pa when stabilizing at a given station-keeping altitude (Fig. 7(a), Fig. 8(a)), this is because the DPD is regulated to compensate the altitude difference only, the platform will restore its original over-pressure state to satisfy the lift and gravity balance condition as it reached the target altitude.

4.3.2 Factors affecting flow rate analysis

The real blower flow rate (air mass change rate) is dependent on the altitude variation and pressure difference variation as described in Eq. (12), so:

$$dm_a = \rho_a V_a \left(1 + \frac{\delta P_a}{P} \right) \Big|_h - \rho'_a V'_a \left(1 + \frac{\delta P'_a}{P'} \right) \Big|_{h'} \quad (17)$$

Eq. (17) is a multivariate expression and no ana-

lytical solution. So the factors affecting flow rate are studied by simulations. In this section only altitude regulation phases are taken into consideration, so open ascending phase from ground to 20 km is not shown in the following simulation results.

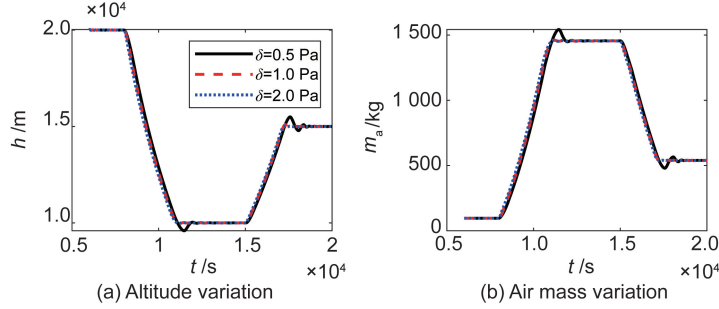


Fig. 9 Altitude and remaining air mass with different PDTs

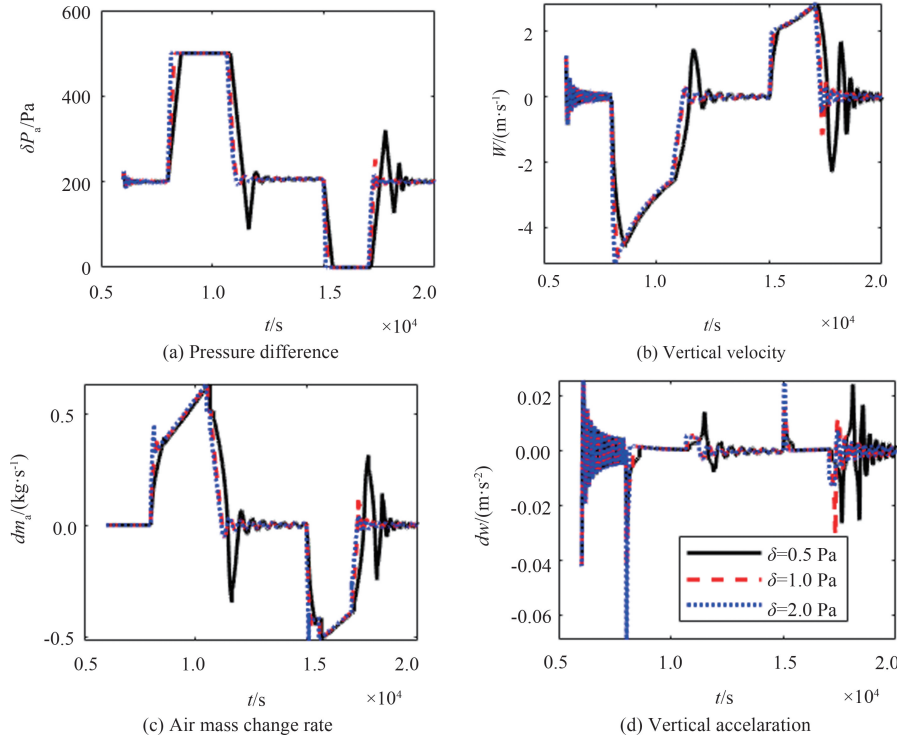


Fig. 10 State variations with different PDTs

There are not obvious differences in altitude regulation and remaining air mass with different PDTs, as shown in Fig. 9. The other states is shown in Fig. 10. There are different maximum values of vertical speed, accelerations and blower flow rates when the commands is switched, where the PDT of $\delta = 10$ Pa induces more abrupt changes in acceleration and blower flow rate when the pressure difference has sudden change; the PDT of $\delta = 0.5$ Pa induces more oscillation at the station keeping altitude. So reasonable choice of PDT helps improve the control quality, however it does not affect the overall altitude control results. It demon-

strates the robustness of the controller. The blower flow rate is decided by the PDT δ directly. Here $\delta = 0.5$ Pa, $\delta = 2$ Pa and $\delta = 10$ Pa are given for evaluating the relationship of PDT with blower flow rate, as shown in Figs 9 and 10.

strates the robustness of the controller.

Comparison of Fig. 9(a) with Fig. 10(a) indicates that in the descending phase, the pressure difference reaches the maximum of 500 Pa to descend. In the ascending phase, the pressure difference reaches the minimum of 0 Pa to ascend. Thus, the vertical acceleration regulation ability is decided not only by the blower flow rate, but also by the designed margin of pressure difference (MPD). MPD is the difference of the designed pressure difference with the maximum or minimum pressure difference.

Here $\Delta P_{\max} = 500$ Pa, $\Delta P_{\max} = 400$ Pa, $\Delta P_{\max} =$

300 Pa, which are corresponding to MPD = 300 Pa, MPD = 200 Pa, MPD = 100 Pa, are given for evaluating the relationship of MPD with blower flow rate, as shown in Figs 11 and 12. The flow rate, vertical speed and vertical acceleration are related with MPD closely.

With increase of the MPD, the flow rate, vertical speed and vertical acceleration are increasing. Thus the transition time for altitude tracking and air mass change rate are different.

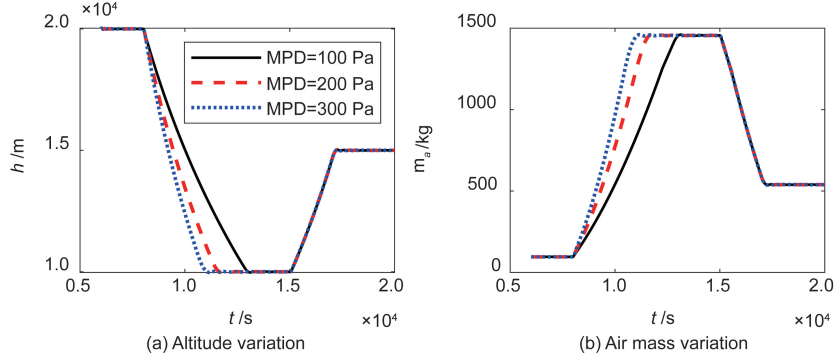


Fig. 11 Altitude and remaining air mass with different MPDs

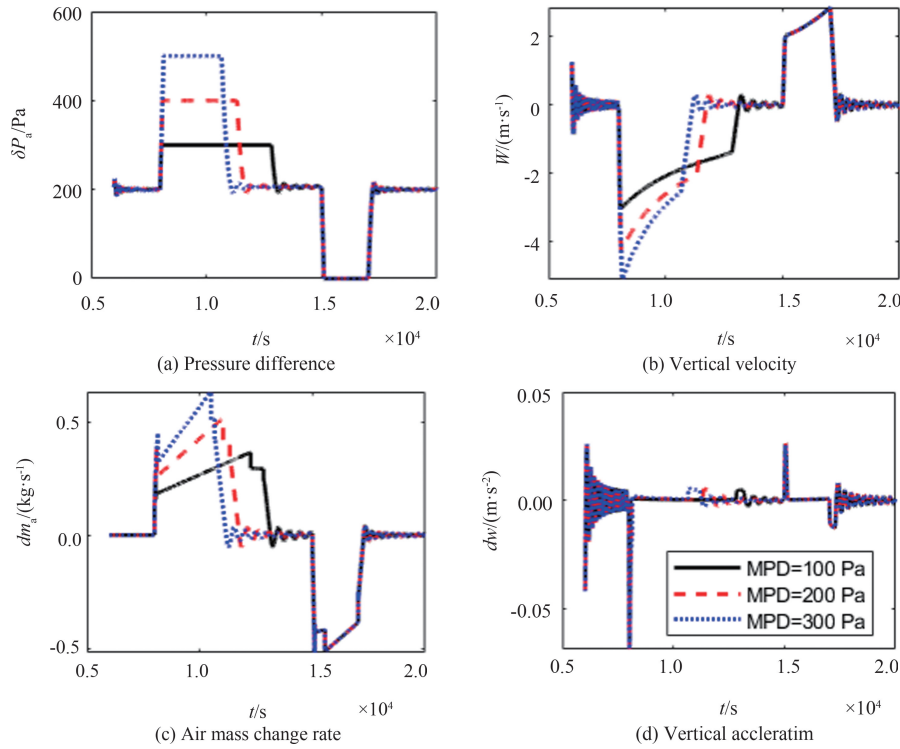


Fig. 12 State variations with different MPDs

4.3.3 Altitude tracking with vertical wind disturbance

In order to verify the tracking stability of DPD as a control variable, the random vertical wind disturbance with maximum amplitude of $3 \text{ m} \cdot \text{s}^{-1}$ is given as shown in Fig. 13, and the state variations and altitude tracking results are shown in Fig. 14.

From Fig. 13, it can be seen that the vertical wind induced vertical drag on the airship, causing the vertical acceleration disturbance to oscillate between $\pm 0.5 \text{ m} \cdot \text{s}^{-2}$ (Fig. 14(f)), the controller makes air

mass exchange frequently to resist the disturbance (Fig. 14 (d)), as a result the altitude tracking is smooth as before. So the designed controller has strong anti-interference ability.

5 Conclusions

Altitude adjustment of a StratoSat is carried out with DPD as the control variable. The pressure difference change threshold is set based on the ability of the

blower, and the control command is switched in accordance with the threshold to realize blower flow control. Then, the altitude is adjusted autonomously. The vertical regulation ability is decided by the blower flow rate and the designed MPD.

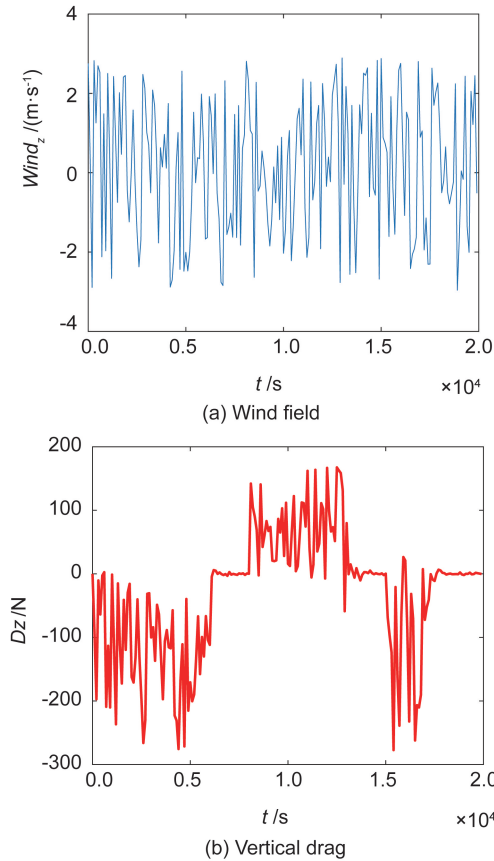


Fig. 13 Vertical wind and vertical drag disturbance

Different factors affecting the control ability are analyzed by simulations. This controller can keep constant pressure difference at arbitrary station-keeping altitude. Compared with altitude as the control variable, the control variable in this scheme is DPD, which is a slow-varying variable. It can maintain a high tracking accuracy by avoiding the complexity of model calculation, at the same time, the control response to differential pressure difference is delayed, and the overshoot caused by the large inertia of the platform is inhibited, which is suitable for the motion control of large-mass vehicles, such as StratoSat, within a wide range of altitude regulation. Therefore, the designed controller has strong anti-interference ability and is suitable for engineering applications.

This controller is based on the assumption that the pressure difference between the helium balloon and ballonet is equal under the steady state, thereby ignoring the transition time of gas expansion and compres-

sion. The commanded pressure difference is decided by the volume ratio, atmosphere density, and pressure at the target altitude, which may be inaccurately determined. Thus, future work could establish an experimental model of atmosphere density and pressure in relation to altitude in a certain experimental area to eliminate altitude errors when the commanded pressure difference is reached.

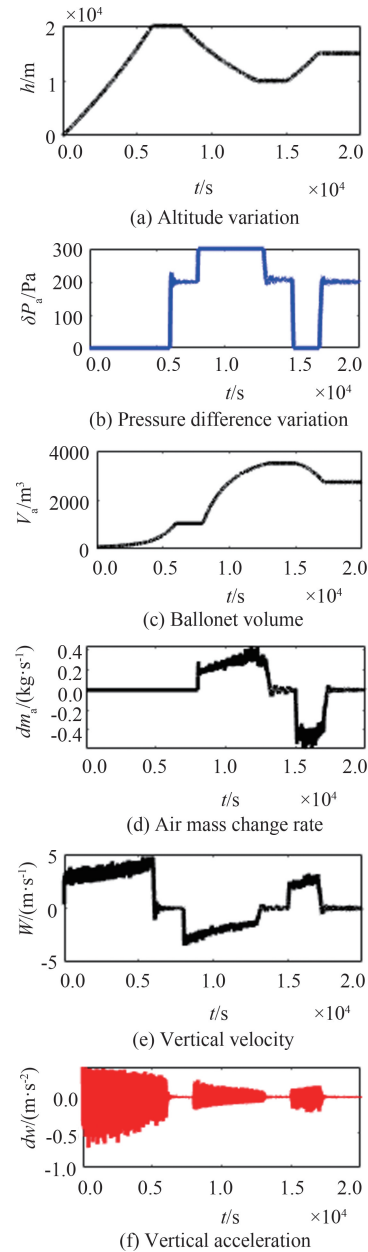


Fig. 14 State variations with vertical wind disturbance

References

[1] D' OLIVEIRA F A, FRANCISCO C L, TESSALENO C D. High-altitude platforms present situation and technology trends [J]. Journal of Aerospace, Technology and Management, 2016, 8(3):249-262.

- [2] ZAUGG E C, MARGULIS A, BRADLEY J P, et al. SAR imaging from stratospheric balloons: first results [C] // 2019 IEEE Radar Conference. Boston, USA: IEEE, 2019: 1-6.
- [3] PANKINE A, LI Z Q, PARSONS D, et al. Stratospheric satellites for earth observations [J]. American Meteorological Society, 2009, 90(8): 1109-1119.
- [4] BUGGA R, JONES J P, PAUKEN M. Extended-range variable altitude balloons for venus atmospheric missions [J]. Acta Astronautica, 2022, 197: 69-80.
- [5] VANDERMEULEN I, GUAY M, MCLELLAN P J. Formation control of high-altitude balloons by distributed extremum seeking control [C] // American Control Conference. Boston, USA: IEEE, 2016: 2524-2529.
- [6] AARTI, UPASNA. Review on project loon [J]. International Journal of Engineering Research & Technology, 2017, 5(3): 1.
- [7] RENATO A B, SIMONE B, CHANTAL C, et al. Altitude control of a remote-sensing balloon platform [J]. Aerospace Science and Technology, 2021, 110: 1-7.
- [8] DAI Q M, FANG X D, LI X J, et al. Performance simulation of high altitude scientific balloons [J]. Advances in Space Research, 2012, 49(6): 1045-1052.
- [9] SHI H, GENG S S, QIAN X H. Thermodynamics analysis of a stratospheric airship with hovering capability [J]. Applied Thermal Engineering, 2019, 146: 600-607.
- [10] MENG J H, ZHANG L C, LI J, et al. Dynamic modeling and simulation of tethered stratospheric satellite with thermal effects [J]. Applied Thermal Engineering, 2017, 110: 181-189.
- [11] ZUO Z Y, SONG J W, ZHENG Z W, et al. A survey on modelling, control and challenges of stratospheric airships [J]. Control Engineering Practice, 2022, 119: 1-10.
- [12] SCHMIDT D K. Modeling and near-space station-keeping control of a large high-altitude airship [J]. Journal of Guidance, Control, and Dynamics, 2007, 30(2): 540-547.
- [13] LEE S J, LEE H. Backstepping approach of trajectory tracking control for the mid-altitude unmanned airship [C] // AIAA Guidance, Navigation and Control Conference and Exhibit. Hilton, USA: AIAA, 2007: 1-14.
- [14] CHEN L, ZHOU G, YAN X J, et al. Composite control of stratospheric airships with moving-masses [J]. Journal of Aircraft, 2012, 49(3): 794-801.
- [15] CHEN L, DUAN D P. Attitude control of stratospheric airship with ballonets and elevator [C] // Proceedings of the 32nd Chinese Control Conference. Xi'an, China: CCC, 2013: 4255-4258.
- [16] CHEN L, DONG Q, ZHANG G C, et al. Composite control system of hybrid-driven mid-altitude airship [J]. The Aeronautical Journal, 2018, 122(1248): 173-204.
- [17] WANG Y, ZHENG G, EFIMOV D, et al. Differentiator application in altitude control for an indoor blimp robot [J]. International Journal of Control, 2018, 91(9): 2121-2130.
- [18] MANSUR A, LANTEIGNE E. Altitude trajectory control of an unmanned airship using incremental nonlinear dynamic inversion [C] // Proceedings of the Canadian Society for Mechanical Engineering International Congress. Charlottetown, Canada: CSME, 2020: 21-24.
- [19] AZINHEIRA J R, MOUTINHO A D, PAIVA E C. Airship hover stabilization using a backstepping control approach [J]. Journal of Guidance, Control, and Dynamics, 2006, 29(4): 903-914.
- [20] NIE C Y, ZHU M, ZHENG Z W, et al. Mode-free altitude control for airship based on Q-learning and CMAC network [C] // Proceedings of 2016 IEEE Chinese Guidance, Navigation and Control Conference. Nanjing, China: IEEE, 2016: 12-14.
- [21] HOU Y, YANG J. Height-control scheme of stratospheric airship ascending stage [J]. Ordnance Industry Automation, 2011(3): 73-76 (In Chinese).
- [22] WU L, LI Y, LI Z B. Coordinated control strategy of pressure difference and height of stratospheric airships [J]. Journal of Central South University (Science and Technology), 2011(42): 328-335 (In Chinese).

CHEN Li, born in 1975. She received her Ph. D degree in Shenyang Institute of Automation in 2004. She also received her B. S. and M. S. degrees from Northeast University in 1994 and 2001 respectively. Her research interests include flight control, mechanics and robot slam.